Methane emissions in seagrass meadows as a small offset to carbon sequestration

Yvonne Yu Yan Yau[1], Gloria Reithmaier[2], Claudia Majtenyi-Hill[1], Nerea Piñeiro-Juncal[3], Martin Dahl[2], Miguel Angel Mateo[4], Stefano Bonaglia[1], Oscar Serrano[5], and Isaac Santos[1]

[1]University of Gothenburg
[2]Unknown
[3]University of Aveiro
[4]Consejo Superior Investigaciones Cientificas
[5]Edith Cowan University

December 14, 2022

Abstract

Seagrass meadows are effective carbon sinks due to their high primary production and sequestration in sediments. However, methane (CH4) fluxes can partially counteract their carbon sink capacity. Here, we measured diffusive sediment-water and air-sea CO2 and CH4 fluxes in a coastal embayment dominated by Posidonia oceanica in the Mediterranean Sea. High resolution timeseries observations revealed large spatial and temporal variability in CH4 concentrations (2 to 36 nM). Higher emissions were observed in an area with dense seagrass meadows. A 6 - 40% decrease of CH4 concentration in the surface water around noon indicates that photosynthesis likely limits CH4 fluxes. Sediments were the major CH4 source as implied from radon (a natural porewater tracer) observations and evidence for methanogenesis in deeper sediments. CH4 sediment-water fluxes (0.1 ± 0.1 - 0.4 +- 0.1 µmol m-2 d-1) were higher than average water-air CH4 emissions (0.12 ± 0.10 µmol m-2 d-1), suggesting that dilution and CH4 oxidation in the water column could reduce net CH4 fluxes into the atmosphere. Overall, relatively low air-sea CH4 fluxes at this likely represent net emissions from subtidal seagrass habitats sites, which are not influenced by nearby allochthonous CH4 sources. The local CH4 emissions in P. oceanica offset less than 1% of the carbon burial in sediments (142 ± 69 g CO2eq m-2 yr-1). Combining our results with earlier observations in other seagrass meadows worldwide reveals that global CH4 emissions within seagrass meadows only offset a small fraction (<2%) of carbon sequestration in sediments.

Hosted file

950175_0_art_file_10525187_rmtb30.docx available at https://authorea.com/users/566175/articles/612952-methane-emissions-in-seagrass-meadows-as-a-small-offset-to-carbon-sequestration

Methane emissions in seagrass meadows as a small offset to carbon sequestration

Yvonne Y.Y. Yau[1], Gloria Reithmaier[1], Claudia Majtenyi-Hill[1], Oscar Serrano[2,3], Nerea Piñeiro-Juncal[2,4], Martin Dahl[2,6], Miguel Angel Mateo[2,3], Stefano Bonaglia[1], and Isaac R. Santos[1, 7]

[1] Department of Marine Sciences, University of Gothenburg, Gothenburg, Sweden

[2] Centro de Estudios Avanzados de Blanes, Consejo Superior de Investigaciones Científicas, Blanes, Spain

[3] School of Science and Centre for Marine Ecosystems Research, Edith Cowan University, Joondalup, WA, Australia

[4] Department of Biology & CESAM – Centre for Environmental and Marine Studies, University of Aveiro, Aveiro, Portugal

[5] CRETUS, EcoPast (GI-1553), Facultade de Bioloxía, Universidade de Santiago de Compostela, Campus Sur s/n, Santiago de Compostela, 15782, Spain

[6] Södertörn University, School of Natural Sciences, Technology and Environmental Studies, Environmental Science. Stockholm University, Sweden

[7] National Marine Science Centre, Southern Cross University, Australia

Corresponding author: Yvonne Yu Yan Yau (yvonne.yau@gu.se)

Key Points:

- High resolution CH_4 observations reveal diel cycles linked to seagrass productivity
- Sediments were the main CH_4 source in both living and dead seagrass areas
- CH_4 emissions were a small offset to seagrass C sequestration on local and global scales

Abstract

Seagrass meadows are effective carbon sinks due to their high primary production and sequestration in sediments. However, methane (CH_4) fluxes can partially counteract their carbon sink capacity. Here, we measured diffusive sediment-water and air-sea CO_2 and CH_4 fluxes in a coastal embayment dominated by *Posidonia oceanica* in the Mediterranean Sea. High resolution timeseries observations revealed large spatial and temporal variability in CH_4 concentrations (2 to 36 nM). Higher emissions were observed in an area with dense seagrass meadows. A 6 − 40% decrease of CH_4 concentration in the surface water around noon indicates that photosynthesis likely limits CH_4 fluxes. Sediments were the major CH_4 source as implied from radon (a natural porewater tracer) observations and evidence for methanogenesis in deeper sediments. CH_4 sediment-water fluxes ($0.1 \pm 0.1 - 0.4 \pm 0.1$ µmol m^{-2} d^{-1}) were higher than average water-air CH_4 emissions (0.12 ± 0.10 µmol m^{-2} d^{-1}), suggesting that dilution and CH_4 oxidation in the water column could reduce net CH_4 fluxes into the atmosphere. Overall, relatively low air-sea CH_4 fluxes at this likely represent net emissions from subtidal seagrass habitats sites, which are not influenced by nearby allochthonous CH_4 sources. The local CH_4 emissions in *P. oceanica* offset less than 1% of the carbon burial in sediments (142 ± 69 g CO_{2eq} m^{-2} yr^{-1}). Combining our results with earlier observations in other seagrass meadows worldwide reveals that global CH_4 emissions within seagrass meadows only offset a small fraction (<2%) of carbon sequestration in sediments.

Plain language Summary

Seagrass meadows are important hotspots for carbon storage in the sediment. Part of the sediment carbon can be emitted as the greenhouse gases carbon dioxide and methane (CH_4). Methane has a 45 – 96 times more powerful global warming effect than carbon dioxide. If seagrass meadows release CH_4, the emissions counteract their climate mitigation potential. We measured greenhouse gas concentrations and fluxes in a seagrass-dominated Mediterranean embayment. Low CH_4 coincided with the increase of oxygen produced through seagrass photosynthesis. Areas with dense seagrass meadows had lower CH_4 emissions. Overall, the seagrass-dominated bay was a small source of CH_4 that can offset only <1% of carbon buried in sediments. Hence, seagrass meadows remain an effective carbon sink.

1 Introduction

Seagrass meadows are effective carbon sinks recognized for their potential role in climate change mitigation (Fourqurean et al., 2012; Lovelock & Duarte, 2019; Mcleod et al., 2011). Seagrass meadows sequester carbon dioxide (CO_2) through photosynthesis (Van Dam et al., 2021) and trap allochthonous particles within their canopy (Gacia et al., 2002). Part of this carbon is then stored as biomass and as organic carbon in sediments for centuries and even millennia (Serrano et al., 2016, 2021). Seagrass meadows account for 10 – 18% of the total carbon burial (27 44 Tg C y^{-1}) in the ocean even though they cover only 0.1% of the global ocean area (Kennedy et al., 2010). In addition, about 5% of the particulate organic carbon and dissolved organic carbon produced within seagrass habitats is exported beyond the meadows and stored in the deep ocean (Duarte & Krause-Jensen, 2017). Seagrass meadows are considered an important blue carbon ecosystem that should be protected and restored to mitigate anthropogenic CO_2 emissions

Posidonia oceanica is the dominant seagrass species along the Mediterranean coast and an important blue carbon ecosystem (Telesca et al., 2015). *P. oceanica* is a slow-growing and long-living seagrass, which accumulates 84 ± 20 g C m^{-2} yr^{-1} of organic carbon in the sediment (Serrano et al., 2016). A special feature of *P. oceanica* is the formation of thick (up to 6.5 m) and old (up to millennia) organic detritus known as *mattes*, storing large quantities of organic matter in the sediments (Lo Iacono et al., 2008; Mateo et al., 1997). These dead mattes can remain as important carbon and biogeochemical sinks even 30 years after seagrass death of the meadow (Apostolaki et al., 2022). Due to their slow decay rates and recalcitrant nature, *P. oceanica* is one of the largest blue carbon sinks among seagrass species (Gacia et al., 2002; Kaal et al., 2018; Serrano et al., 2018). However, natural and human disturbances such as moorings and coastal development destroy seagrass meadows potentially leading to reduction of carbon stocks and increased emissions of CO_2 and CH_4 to the atmosphere (Carnell et al., 2020; Lyimo et al., 2018).

The coastal ocean is a hotspot of CH_4 emissions, contributing with 75% of the global oceanic CH_4 emissions (Weber et al., 2019). While seagrass meadows store organic carbon, the high sediment organic matter content also favors methane (CH_4) production (Rosentreter, Al-Haj, et al., 2021). CH_4 is produced during anaerobic microbial degradation of organic carbon via methanogenesis (Martens & Klump, 1980) usually after all the other energetically favorable electron acceptors become depleted in sediments (Froelich et al., 1979). Thus, oxygen, nitrate, metal oxide and sulphate availability in marine sediments can limit methanogenesis and CH_4 emissions (Egger, Kraal, et al., 2016). The presence of methylated compounds in seagrass rhizosphere provide another pathway for CH_4 production, even in dead seagrass meadows (Schorn et al., 2022). The net CH_4 emission is also controlled by production and oxidation in sediment and water column before reaching the atmosphere (Egger, Lenstra, et al., 2016; Ward et al., 1987). Understanding both sediment-water and air-sea fluxes can provide insight on net CH_4 fluxes to the atmosphere.

Since CH_4 is a potent greenhouse gas with 45–96 times greater sustained-flux warming potential (SGWP) than CO_2 (Neubauer & Megonigal, 2015), the efficiency of seagrasses as a carbon sink can be partially offset by CH_4 emissions. Although measurements of CH_4 fluxes

have been widely performed in mangroves (Call et al., 2019), saltmarshes (Yau et al., 2022), and other coastal ecosystems (Borges & Abril, 2011), CH_4 fluxes in seagrass meadows remain poorly constrained across multiple spatial and temporal scales. The air-sea and sediment-water CH_4 fluxes from seagrass ranged from 0 to 400 μmol m^{-2} d^{-1}, resulting in global upscaled fluxes of 0.18 Tg CH_4 per year (Al-Haj et al., 2022). Several seagrass meadow CH_4 flux estimates considered sediment-water fluxes, obtained from benthic chambers and sediment incubation approaches, to be equivalent to air-sea fluxes. This assumes that sediment CH_4 propagates through the shallow water column and reaches the atmosphere unmodified.

Here, we report high resolution timeseries observations of dissolved CH_4 over multiple diel cycles and estimate sediment-water and air-sea CH_4 fluxes in *P. oceanica* meadows at a Mediterranean bay. We quantified air-sea CO_2 and CH_4 fluxes above the seagrass using automated, *in situ* surface water observations (including ^{222}Rn measurements, a natural porewater tracer), and at the sediment-water interface using sediment cores. This study aims to (1) estimate sediment-water CH_4 fluxes, (2) evaluate the spatial and diel variability of air-sea CH_4 fluxes, (3) assess the fate of CH_4 by comparing CH_4 sediment-water fluxes and air-sea fluxes, and (4) examine whether CH_4 emissions can partially offset carbon sequestration in seagrass on both local and global scales.

2 Materials and Methods

2.1Sampling location

Field observations were performed at Portlligat Bay (42°17’32” N, 3°7’28” E) on the northeast coast of Spain in the Mediterranean Sea. The bay is shallow ranging from 2 to 10 m, with < 0.5 m tidal ranges (Serrano et al., 2012). *P. oceanica* is the dominant seagrass species in the bay, covering 41% of the area (0.12 km^2). The seabed is irregular with mounds of matte deposits (ranging from 3.5 to 6 m in thickness) formed by *P. oceanica* debris intertwined with fine to medium sands (Lo Iacono et al., 2008). Dense *P. oceanica* (> 600 shoots m^{-2}) were found within the center and north of the bay, whereas patchy seagrass meadows within sand and dead mattes were found at the south of the bay. Anthropogenic disturbances in the embayment are limited to boating and the deployment of environmentally friendly moorings in the center of the bay. The nature of the matte with the presence of dense roots, rhizomes and sheaths remains of *P. oceanica* limits burrowing activities in the sediments. An ephemeral stream is located at the northeast edge of the bay, but there are no permanent rivers supplying freshwater to the bay.

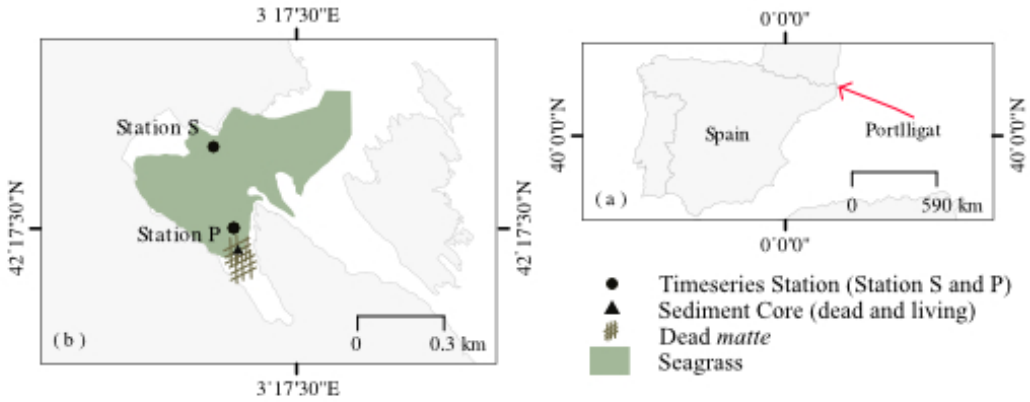

Figure 1. Study site map. (a) Location of Portlligat bay; (b) Portlligat bay with location of timeseries Stations S and P, sediment core of living and dead seagrasses, extent of *Posidonia oceanica* meadows (shaded green) modified from (Leiva-Dueñas et al., 2018) and the dead *matte*.

2.2Timeseries and spatial survey

Two timeseries stations were deployed simultaneously during 11th to 18th September 2021 (Figure 1). Station S was in a healthy seagrass-dominated area (42°17'38" N, 3°17'19 E"), whilst Station P was surrounded by patchy seagrass meadows, including dead seagrass areas (42°17'29" N, 3°17'22 E"). Precipitation events were recorded from 01:00 to 09:00 on 16th September with a maximum 2.9 cm hr^{-1}.

Water depth, salinity and temperature were measured every 5 minutes (Levelogger 5 LTC, Solinst), whereas dissolved oxygen (DO) was recorded at 1 min intervals (miniDOT, PME), which were installed close to the sediment surface. Radon was measured with a ^{222}Rn-air analyzer (RAD7), while CO_2 and CH_4 were measured with a greenhouse gas analyzer (LI-7810, LI-COR). Both were connected to a Durridge shower head gas exchange device as described elsewhere (Webb et al. 2016 and references there in). A water pump was attached at the side of the boat (~50 cm deep) to sample surface water at 3 L min^{-1} to the showerhead gas exchange. There were data gaps in the patchy seagrass due to instrument failure (days 13th and 14th September 2021). CO_2 and CH_4 concentrations were recorded at 1-second intervals and radon at 30 min intervals. Time lags of 30, 10 and 30 minutes were applied to ^{222}Rn, CO_2 and CH_4 respectively to account for gas equilibrium between water and the closed air loop (Webb et al., 2016). The data were aggregated into 5 minutes intervals.

A spatial survey was conducted to measure ^{222}Rn, CO_2 and CH_4 across the bay covering a track of 1.5 km on 18th September 2021 from 16:00 to 17:30 using the same experimental setup as described above. CH_4 fluxes for the whole bay area were found using inverse distance weighted interpolation methods, from which an average was obtained.. Solubility of CO_2 and CH_4 was calculated as a function of temperature and salinity using Weiss (1974) and Yamamoto et al. (1976), respectively, and normalized to the Schmidt number as described in Wanninkhof (2014). Meteorological parameters such as radiation, wind speed and

precipitation were obtained from nearest automated station of Roses (42° 16' 20.56" N, 3° 11' 1.16" E) from the government of Catalonia.

2.3 Sediment and porewater analysis

Six sediment cores were collected by manual hammering of PVC pipes (1 m long and 60 mm inner diameter) in both dead and living seagrass (Figure 1). To sample for dissolved CH_4 in porewater, a push-core with pre-drilled holes (1 cm diameter) was used to minimize the oxidation during sampling. 3mL of wet sediment were extracted using a cut-off plastic syringe and transferred into 22mL gas-tight vials containing 10 mL of a 1M NaOH solution to preserve methane. The vials were then crimped immediately using aluminum caps with butyl rubber stoppers. Back in the lab, all headspace from each vial (7–10 mL) were transferred into a second N_2 flushed vial using a gas-tight syringe. The headspace CH_4 concentrations were then measured using a gas chromatographer (Thermo Scientific Trace 1300) equipped with flame ionization detector. Reference gas standards of 1.9 ppm and 50 ppm (Air Liquide Gas AB) were used for instrument calibration. The porewater methane concentrations were calculated from the measured headspace concentrations (Hoehler et al., 2000), (Equation 1):

$$[CH_4] = \frac{P * V_H}{R * T * \emptyset * V_S} \qquad (1)$$

where $[CH_4]$ is the porewater CH_4 concentration (nM), P is the methane partial pressure inside the vial (atm), V_H and V_S are the volume of headspace in each vial and the sediment sample (mL), R is the universal gas constant (L atm K^{-1} mol^{-1}), T is the laboratory temperature (°C) and $\emptyset$ is the sediments porosity in each sediment layer. Sediment porosity was calculated from water content (weight difference of wet and dry sample weight after drying at 100°C) and sediment bulk density (Lengier et al., 2021)

Porewater for DIC was extracted from sediment cores using Rhizon samplers (Rhizosphere research product). Approximately 10–15 mL of porewater was collected. DIC samples were collected in 12 mL exetainers without headspace. DIC concentrations were analyzed by Total Dissolved Inorganic Carbon Analyzer (Appollo AS-C5) at the University of Gothenburg. Certified reference material (CRM from Dickson Laboratory, Scripps Institute of Oceanography) was used as the standard. The analytical precision was better than 2% for porewater.

The organic matter content of the sediment layers was estimated based on the Loss of Ignition method (LOI), after homogenising the samples with a mill and combusting the organic matter for 4h at 500 °C (Heiri et al., 2001).

2.4 Estimation of sediment-water and air-sea CH_4 and CO_2 flux

The sediment-water CO_2 and CH_4 diffusive fluxes were calculated using Fick's first law:

$$J = -\emptyset D_S \frac{dC}{dz} \qquad (2)$$

where J is diffusive flux of CH_4 and DIC (μmol m^{-2} d^{-1}), $\emptyset$ is the sediment porosity, D_S is the sediment diffusion coefficient (cm^2 s^{-1}), C is the CH_4 concentration in porewater (μM) and z

is the sediment depth (cm). The values of $\frac{dC}{dz}$ were obtained from the slope of the linear regressions where $p < 0.05$. The diffusion in sediment (D_S) was adjusted to the diffusion in seawater using sediment tortuosity based on $D_S = \frac{D_{SW}}{\theta}$, where the seawater diffusion coefficient (D_{SW}) for CH_4 and DIC seawater at 20ºC was $1.39*10^{-9}$ and $9.89*10^{-10}$ (Lerman, 1979). Tortuosity (θ) was calculated from sediment porosity using $\theta = 1 - In(\emptyset^2)$ (Boudreau, 1997; Lengier et al., 2021).

The air-sea CO_2 and CH_4 fluxes were determined by gradient of air-sea gas concentration, gas solubility and gas transfer velocity (Equation 1).

$$FCH_4 \,/\, FCO_2 = k\, k_0(P_W - P_a) \qquad (3)$$

where F is the CO_2 and CH_4 flux (mmol m^{-2} d^{-1}), k represents gas transfer velocity (m d^{-1}), k_0 is the solubility coefficient (mol kg^{-1} atm^{-1}), and P_w and Pa are the partial pressures (µatm) of CO_2 and CH_4 in water and air, respectively. The atmospheric partial pressures of CO_2 and CH_4 were 419 and 1.9 ppm, respectively. Positive air-sea gas flux values indicate gas evasion from water to air. Four empirical models were used to determine the gas transfer velocity k, which was based on the water depth and wind speed at 10 m above sea level (m s^{-1}) (Borges et al., 2004; Dobashi & Ho, 2022; Raymond & Cole, 2001; Wanninkhof, 2014) (Table 1). These models were selected for intermediate wind speed of 3–15 m s^{-1}. Dobashi and Ho (2022) model was determined in seagrass in Florida Bay, which accounted for the wave resistance by seagrass and lower wind fetch in meadows. Dobashi and Ho (2022) model for the analysis as it is more suitable for our coastal bay and prevents overestimation of fluxes.

Table 1. *Models for gas transfer velocity parameterizations. k is normalized to Schmidt number (k_{600}) as a function of temperature and salinity.*

Model	**Parameters**	**Location**	**Equation**
Raymond & Cole (2001)	Wind speed	River and estuary	$k_{600} = 1.91e^{0.35u_{10}}$
Borges et al., (2004)	Wind speed	Estuary	$k_{600} = 5.141{u_{10}}^{0.758}$
Wanninkhof (2014)*	Wind speed	River	$k_{660} = 0.251{u_{10}}^{2}$
Dobashi and Ho (2022)	Wind speed	Seagrass	$k_{600} = 0.125{u_{10}}^{2}$

Note. u_{10} is the wind speed at 10 m height (m s^{-1}). *k_{660} is converted to k_{600} for comparison by assuming that both the Schmidt number had the same ratio and exponent of -0.5.

To evaluate the global warming potential, CH_4 flux was converted to CO_2 equivalents. CH_4 flux estimates were based on the sustained-flux global warming potential (SGWP) 96 and 45 for time horizons of 20 and 100 years, respectively (Al-Haj & Fulweiler, 2020; Neubauer & Megonigal, 2015). The CO_2 equivalent emissions of CH_4 were calculated as follows:

$$SGWP_{100/20}(Tg\ CO_{2-eq}) = FCH_4 * 365 * A * SGWP_{100/20} * f \qquad (5)$$

where FCH_4 represents average CH_4 flux (µmol m^{-2} d^{-1}); A is the area of seagrass (km^2), SGWP of 100 and 20 years of 45 and 96, f is the conversion factor from µmol to Tg

To investigate whether CO_2 and CH_4 fluxes were different between stations, Mann-Whitney tests were used due to the non-normal distributed data. Spearman's Rank-order test was used to determine the correlations between different environmental parameters. All statistical tests were considered significant when $p < 0.05$.

3 Results

3.1 Timeseries observations

The average water temperature and salinity were similar at Stations S and P, with 23.3 ± 0.7 °C (SD) and 36 ± 1 respectively (Figure 2). The water depth ranged from 1.4 to 2.4 m and wind speeds at 10 m above sea level averaged 2.1 ± 1.6 m s^{-1} over the study period. The light intensity under the water was higher in Station P (1747 ± 633 lum ft^{-2}) than Station S (1044 ± 670 lum ft^{-2}). Over diel periods, DO at both Stations S and P was undersaturated (77.9 ± 16.0% and 74.7 ± 18.2%, respectively). DO followed the expected diel pattern with oversaturated and undersaturated conditions during noon and night, respectively. pCO_2 exhibited a diel cycle with a peak around 9 to 10 am and lowest values around 6 pm and was negatively correlated with DO in both stations (Figure 2). The hourly average CH_4 concentrations were significantly different at both sites, with Station P were 5 times higher than Station S. We observed a 40% decrease in CH_4 concentrations from 11:00 to 14:00 at Station P, but only 6% decrease in Station P during noon in Station S. The daytime average wind speed, and the CH_4 and CO_2 fluxes were higher than at nighttime (Table 2). The hourly average of pCO_2 exhibited a clockwise hysteresis loop with DO saturation and CH_4 at both sites and both stations exhibited a weak but significant correlation between DO saturation and CH_4 (Figure 7). The hourly average CH_4 concentration had a hysteretic pattern to light intensity in Station S but a strong correlation in Station P. However, ^{222}Rn did not follow a diel pattern at both stations.

3.2 Spatial variation

pCO_2 and CH_4 were significantly different between the two stations (Figure 6). pCO_2 values at Station S (538 ± 50 µatm), which is surrounded by healthy seagrass meadows, were lower than at Station P (632 ± 103 µatm), which is mostly surrounded by dead *matte* and organic matter debris over sand (Table 2). Similarly, the CH_4 concentrations were five times lower in Station S (2.68 ± 0.17 nM) compared to Station P (8.57 ± 6.72 nM). ^{222}Rn concentration at Station P (383 ± 125 dpm m^3) was also significantly lower than Station S (892 ± 331 dpm m^3) (Figure 2). The high CH_4 concentrations at Station P (peak at 36.3 nM at 13:00) occurred in the first two days of observations coinciding with the high concentrations of ^{222}Rn (peak at 1886 dpm m^3) and high irradiance (6000 lum ft^{-2}) (Figure 3). ^{222}Rn concentrations were positively correlated with CH_4 at Station P ($r = 0.73$) and Station S ($r = 0.51$) and pCO_2 ($r = 0.49$ and $r = 0.32$, respectively) (Figure 6). Net CH_4 emissions were observed in both stations, with one order of magnitude higher CH_4 sea-air fluxes at Station P (1.10 ± 2.29 µmol m^{-2} d^{-1}) compared to Station S (0.10 ± 0.12 µmol m^{-2} d^{-1}) over the study period. Similarly, net release of CO_2 to the atmosphere was up to 2-fold lower in Station S (3.75 ± 2.63 mmol m^{-2} d^{-1}) compared to Station P (6.32 ± 5.59 mmol m^{-2} d^{-1}).

The CH_4 and CO_2 emissions were calculated from four different gas transfer models. CH_4 emissions estimated from Dobashi and Ho (2022) were 2-times, 6-times and 11-times smaller

than those obtained with the other gas transfer models tested: Wanninkhof (2014), Raymond & Cole (2001) and Borges et al., (2004), respectively.

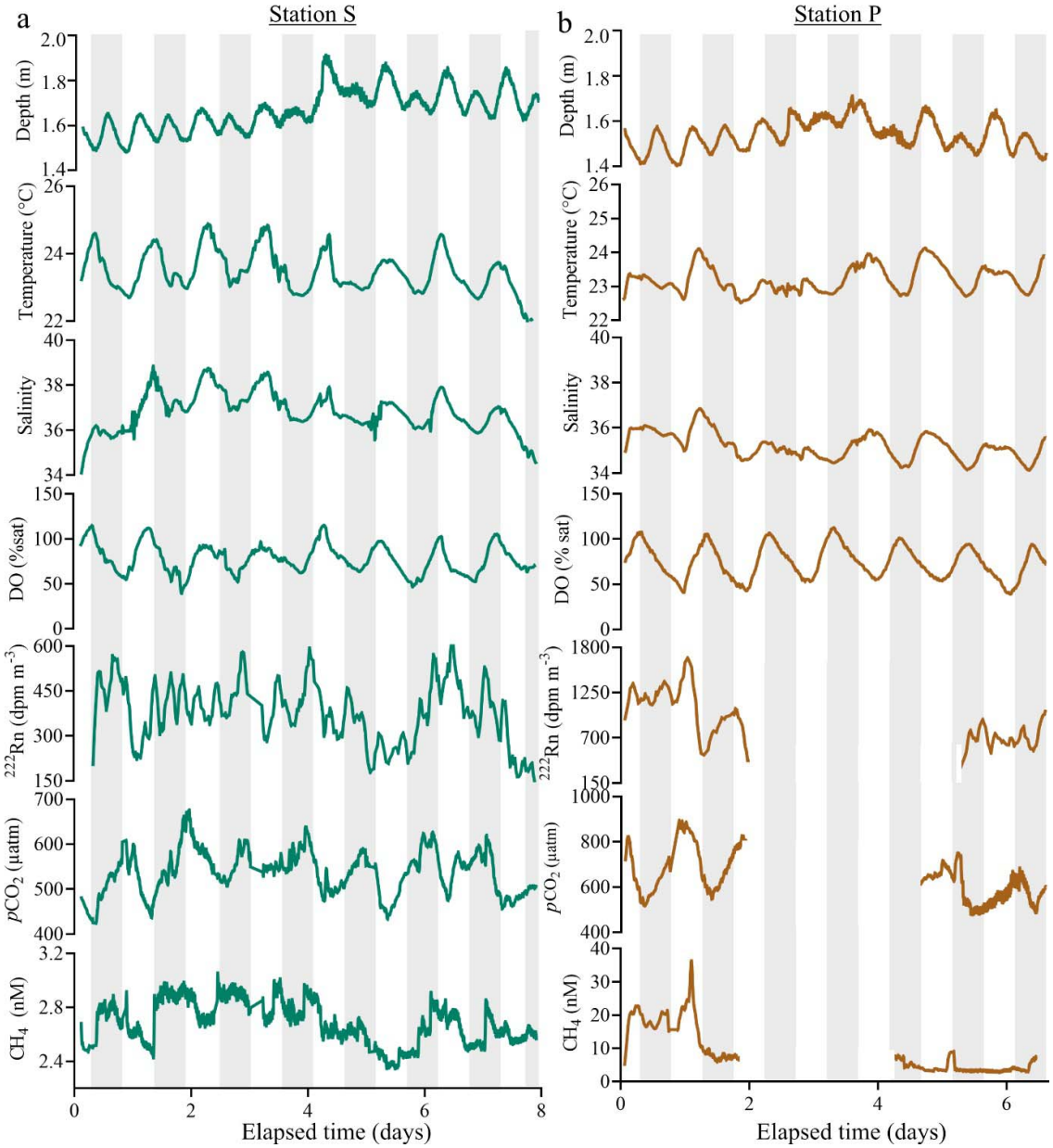

Figure 2. Timeseries observations of dissolved greenhouse gases and ancillary parameters at (a) Station S; and (b) Station P. The shaded area indicates nighttime, whereas the non-shaded area indicates daytime. Gaps in the data were due to instrument failure.

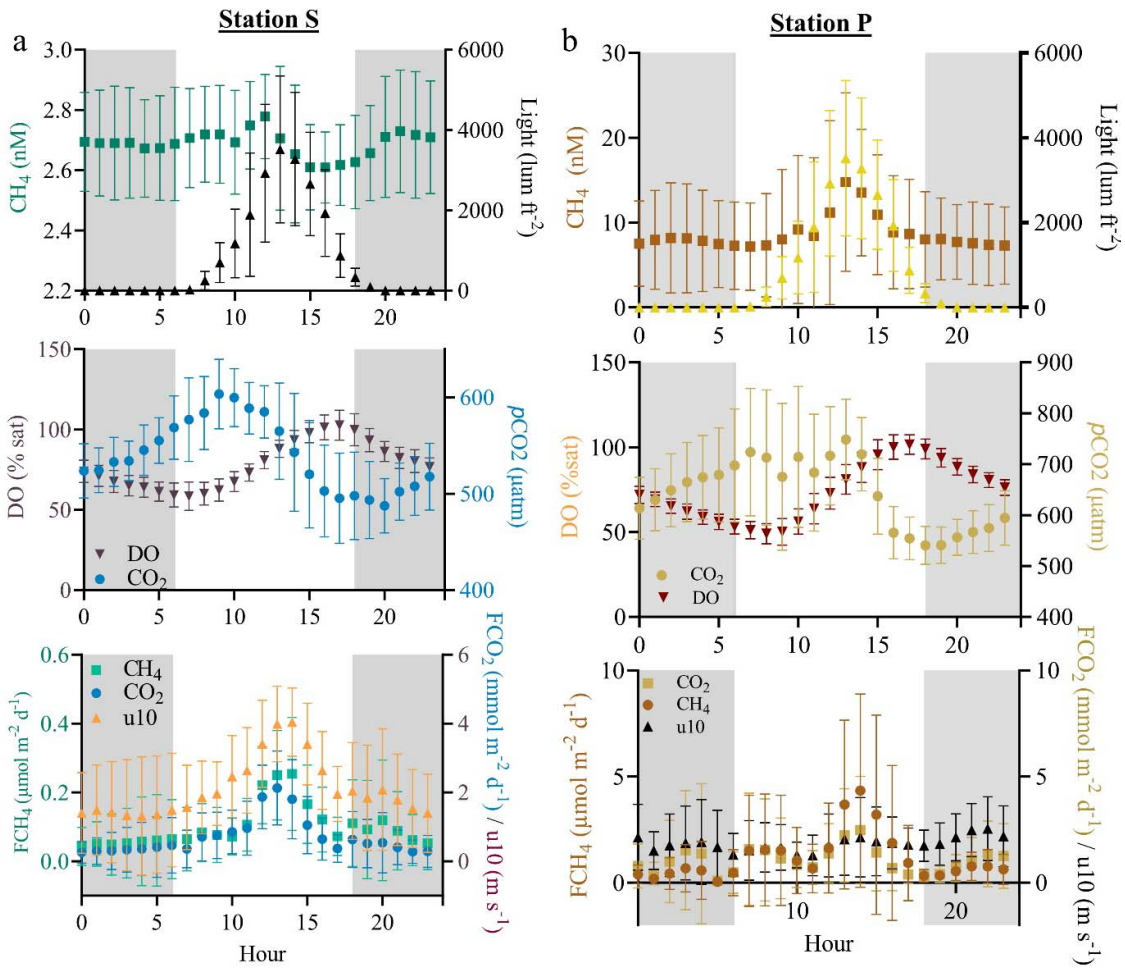

Figure 3. Mean ± standard deviation of hourly concentration of CH_4 (nM), CO_2 (pCO_2), light intensity (lum ft^{-2}), percentage saturation of dissolved oxygen (DO, % sat), wind speed at 10 m above sea level (u10), CO_2 fluxes (FCO_2), and CH_4 fluxes (FCH_4) at Station S (left) and Station P (right) over the period of study. Both CO_2 and CH_4 fluxes were obtained based on the gas transfer model from (Dobashi & Ho, 2022). The shaded area indicates nighttime, whereas the non-shaded area indicates daytime.

Table 2. *A summary of environmental parameters and GHG fluxes measured simultaneously at Station S and Station P.* Day indicates data from 06:00 to 18:00 and night indicates data from 18:00 to 06:00. All data are reported as mean ± SD. The air-sea CO_2 and CH_4 fluxes were calculated from four gas transfer velocity models (R&C from Raymond and Cole 2001; B04 from Borges et al. 2004; W14 from Wanninkhof 2014; and RY22 from Dobashi and Ho 2022).

		Station S			Station P			Spatial Survey
	Unit	Overall	Day	Night	Overall	Day	Night	Overall
Description		*P.oceanica* dominated			Pachy and dead *P.oceanica*			Whole bay
No. of hours	hr	205	97	108	109	61	48	2
Temperature	°C	23.5 ± 0.6	23.0 ± 0.4	23.0 ± 0.3	23.2 ± 0.4	23.1 ± 0.1	23.3 ± 0.1	23.7*
Salinity		36.8 ± 0.9	37 ± 1	37 ± 1	36 ± 1	35 ± 0	35 ± 0	37 ± 0*
Water depth	m	1.7 ± 0.1	1.7 ± 1	1.7 ± 1	1.5 ± 0.1	1.5 ± 0.1	1.5 ± 0.1	1.7*
Wind speed	$m\ s^{-1}$	2.6 ± 1.6	2.6 ± 1.1	1.6 ± 1.4	1.8 ± 1.4	1.7 ± 0.4	1.9 ± 0.4	1.6 ± 0.1*
Irridance	$lum\ ft^{-2}$	526 ± 942	1044 ± 670	18 ± 0	873 ± 1456	1747 ± 633	33 ± 70	/
DO	% Sat	78 ± 16	79 ± 6.8	76 ± 6.5	75 ± 18	74 ± 1	74 ± 1	102 ± 1*
DO	$mg\ L^{-1}$	5.4 ± 1.1	5.4 ± 0.5	5.2 ± 0.4	5.0 ± 1.3	4.5 ± 0.5	5.5 ± 0.4	7 ± 0*
pCO_2	µatm	538 ± 50	561 ± 41	522 ± 27	632 ± 103	677 ± 36	614 ± 20	606 ± 51
CH_4	nM	2.68 ± 0.17	2.69 ± 0.17	2.69 ± 0.19	8.57 ± 6.72	9.82 ± 1.83	7.72 ± 0.72	4.07 ± 1.18
^{222}Rn	$dpm\ m^{-3}$	377 ± 129	392 ± 159	376 ± 130	892 ± 331	863 ± 128	933 ± 81	/
CO_2 flux								
R&C	$mmol\ m^{-2}\ d^{-1}$	3.75 ± 2.63	5.12 ± 2.44	2.81 ± 1.59	6.32 ± 5.59	7.88 ± 2.27	5.53 ± 2.8	4.21 ± 0.84
B04	$mmol\ m^{-2}\ d^{-1}$	7.22 ± 5.27	10.36 ± 4.7	4.91 ± 2.97	11.85 ± 11.05	15.19 ± 4.79	9.96 ± 3.6	9.52 ± 2.01
W14	$mmol\ m^{-2}\ d^{-1}$	1.35 ± 1.78	2.10 ± 1.69	0.82 ± 1.21	2.13 ± 3.58	2.77 ± 1.6	1.75 ± 2.15	0.85 ± 0.20
RY22	$mmol\ m^{-2}\ d^{-1}$	0.64 ± 0.85	1.00 ± 0.76	0.39 ± 0.57	1.01 ± 1.70	1.31 ± 0.76	0.83 ± 1.02	0.38 ± 0.09
CH_4 flux								
R&C	$\mu mol\ m^{-2}\ d^{-1}$	0.56 ± 0.37	0.66 ± 0.36	0.49 ± 0.31	6.59 ± 9.21	9.76 ± 3.18	4.37 ± 0.80	1.33 ± 0.65
B04	$\mu mol\ m^{-2}\ d^{-1}$	1.07 ± 0.71	1.32 ± 0.66	0.87 ± 0.58	12.71 ± 18.73	19.71 ± 5.74	7.75 ± 1.59	2.97 ± 1.47
W14	$\mu mol\ m^{-2}\ d^{-1}$	0.20 ± 0.26	0.28 ± 0.24	0.15 ± 0.21	2.34 ± 4.88	4.24 ± 2.59	1.01 ± 0.83	0.27 ± 0.14
RY22	$\mu mol\ m^{-2}\ d^{-1}$	0.10 ± 0.12	0.13 ± 0.1	0.07 ± 0.1	1.10 ± 2.29	2.00 ± 1.21	0.48 ± 0.39	0.12 ± 0.10

3.3 Spatial survey in the bay

The 2-hour survey across the bay was conducted in late afternoon with wind speed (1.6 $m\ s^{-1}$) lower than the average timeseries measurements (2.2 $m\ s^{-1}$). CH_4 concentrations varied across the bay, ranging from 2.6 to 6.9 nM. The highest CH_4 concentration was detected around Station P and along the SW shoreline, and further decreased towards the east and the opening towards the Mediterranean Sea (Figure 4). This trend is consistent with timeseries observations. Overall, a net release of CH_4 was estimated for the whole bay, ranging from 0.12 ± 0.10 to 2.97 ± 1.47 µmol $m^{-2}\ d^{-1}$, depending on the gas transfer model used. The spatial survey represents the average of whole bay (0.21 km^2), which was 50% higher than the average timeseries measurements recorded at Station S and 91% lower at Station P. For the upscaling of CH_4 emissions, we used the average CH_4 flux for the whole bay to account for the spatial differences.

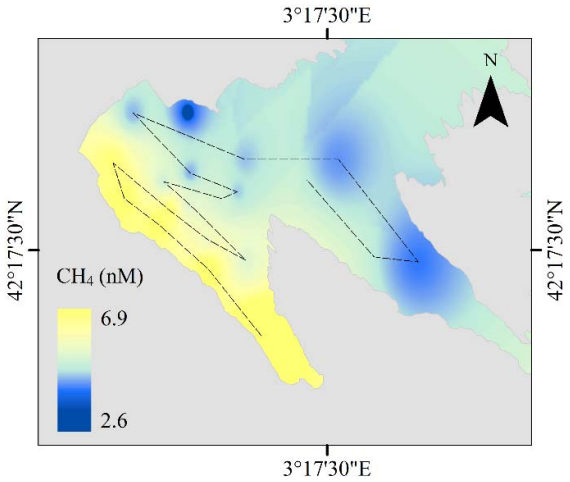

Figure 4. The distribution of CH_4 concentration across Portlligat bay. The dashed black line represents the spatial survey. The northeast exit of the bay is the Mediterranean Sea.

3.4 Porewater profiles

Sediment cores in both living and dead seagrass areas had similar water content ranging from 40% to 55%. Total organic matter content of sediments was similar between cores from living and dead seagrass areas, with an average of 37.9% and 44.3%, respectively (Table 3). Porewater CH_4 concentration in living seagrass cores were two-times higher than in the dead seagrass. Both cores showed similar CH_4 depth profiles, increasing from 1 µM at the surface up to 6 µM at 50 cm (Figure 5). The estimated sediment diffusive CH_4 flux in living seagrass (0.1 – 0.4 µmol m^{-2} d^{-1}) was 2 to 11 times higher than in dead seagrass (0 – 0.1 µmol m^{-2} d^{-1}). CH_4 sediment-water fluxes in the living seagrass were 2.5 times higher than CH_4 air-sea emissions in the Station S (i.e., seagrass-dominated site), whereas sediment-water CH_4 fluxes in the dead seagrass were 0.1 times lower than air-sea emissions in Station P (i.e., a mix of patchy and dead seagrass). Porewater DIC concentrations in living seagrass (1,460 to 8,060 µM) were also two times higher than in the dead seagrass (940 to 5,390 µM) (Table 3). DIC concentration in dead seagrass remained relatively constant with increasing sediment depth, whilst in living seagrass increased steeply up to 30 cm, where the rhizosphere ends, and then after continued to increase until 70 cm depth (Figure 5). The estimated DIC diffusive flux in the living seagrass (185 – 355 µmol m^{-2} d^{-1}) was three-times higher than in the dead seagrass (68 – 88 µmol m^{-2} d^{-1}).

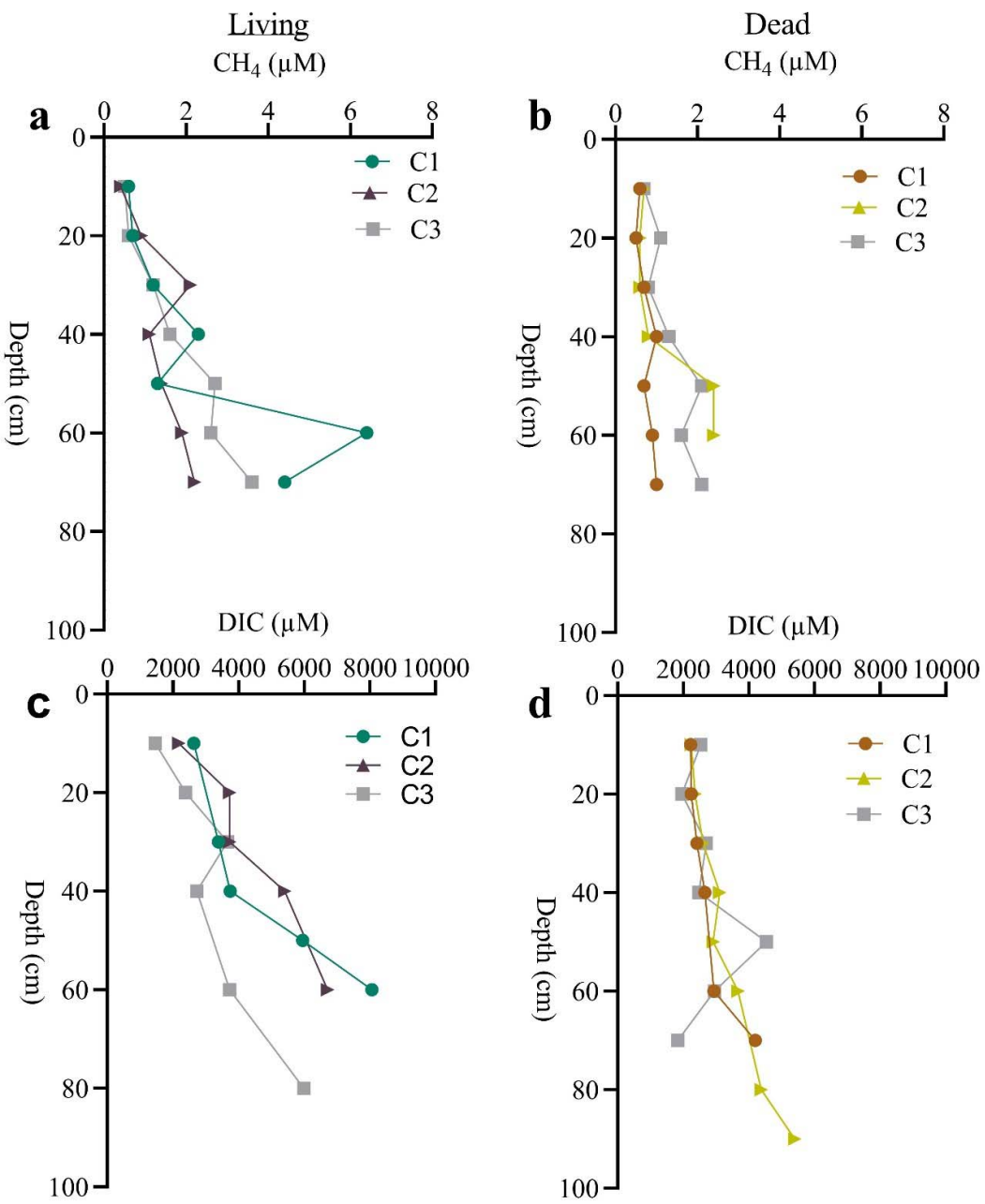

Figure 5. Vertical sediment profiles of porewater CH_4 concentrations (μM) in three replicate cores within a) living meadows and b) dead matte; and DIC concentrations in c) living meadows and d) dead matte.

Table 3. *Sediment characteristics and porewater DIC and CH_4 concentrations in 50cm thick cores from living meadows and dead matte cores. All data are reported as mean ± SD.*

	Unit	Living	Dead
Dry Bulk density[a]	g cm^{-3}	0.2 ± 0.1	0.3 ± 0.1
Water content[a]	%	51 ± 5.1	46 ± 4.9
Particulate Organic matter[a]	%	16.9 ± 7.4	17.5 ± 7.4

DIC	μM	4094 ± 1827	2974 ± 939
CH_4	μM	2.3 ± 1.5	1.1 ± 0.6
CH_4 sediment-water flux	μmol m^{-2} d^{-1}	0.25 ± 0.1	0.1 ± 0.1
DIC sediment-water flux	μmol m^{-2} d^{-1}	280 ± 87	78 ± 15

[a]Average of the first 50 cm of the sediment

4 Discussion

4.1 Porewater methane fluxes

Organic sediments in anoxic conditions support methanogenic activity and can result in high carbon mineralization rates and thus benthic CH_4 effluxes. The high porewater CH_4 concentration (0.3 – 2.1 μM) in both living and dead seagrass sediment, was 20 times higher than previously measured in Italy for the same seagrass species (0.04–0.09 μM), but similar to those estimated for *Zostera noltii* in France (2.5 – 8 μM) (Deborde et al., 2010; Schorn et al., 2022). This might be related to abiotic factors including sediment grain-size distribution (i.e., mud content), and/or the quality and quantity of organic carbon in sediment. The higher CH_4 production below 40 – 50 cm sediments in seagrass sediments compared to the relative flat CH_4 trend in the dead matte could be related to the effects of oxygen pumping by the seagrass rhizosphere on methanogenic activity (Figure 5). The CH_4 consumption could occur in upper layer (Schorn et al., 2022). Positive correlations between the porewater tracer ^{222}Rn and CH_4 concentrations also suggested that the sediments underlying the seagrasses are the main source of CH_4 (and ^{222}Rn) into the environment (Figure 6). There are no other major ^{222}Rn sources such as fresh groundwater or river water input to the bay. Higher sediment-water fluxes than the air-sea water fluxes in dense seagrass (Station S) also implied that the sediment is the source.

High organic carbon in sediments support CH_4 production. A positive relationship between porewater DIC and CH_4 concentrations suggested that methanogenesis supports organic carbon mineralization (Aleksandra & Katarzyna, 2018). Both DIC and CH_4 diffusion rates in the living seagrass were 2–3 times higher than in sediments of dead seagrasses, suggesting that living seagrass releases organic carbon together with O_2 in root exudates, which enhances carbon remineralization rates and thus DIC fluxes (Li, 2021). Living seagrasses, with a higher liable content of labile organic carbon compared to dead *matte* could stimulate the CH_4 production (Piñeiro-Juncal et al., 2021), which was also observed in sediments with *Z. noltii*, which had four-times higher fluxes than bare sediments (Bahlmann et al., 2015). However, based on the sediment CH_4: DIC, the contribution of methanogenesis to total carbon mineralization was at maximum 0.03%.

Our CH_4 diffusive sediment-water flux in living and dead *P.oceanica* of (0.2 μmol m^{-2} d^{-1} and 0.08 μmol m^{-2} d^{-1}, respectively) at Portlligat Bay was 2 orders of magnitude lower than the fluxes measured in Fetoviaia Bay (median of 106 μmol m^{-2} d^{-1} living; 142 μmol m^{-2} d^{-1} for dead) (Schorn et al., 2022), using core incubations. While the flux may not be directly comparable due to different methods, both studies supported the hypothesis that dead *P.oceanica* could accumulate CH_4 due to the production of methylated compounds that fuels methanogenesis (Schorn et al. 2022).

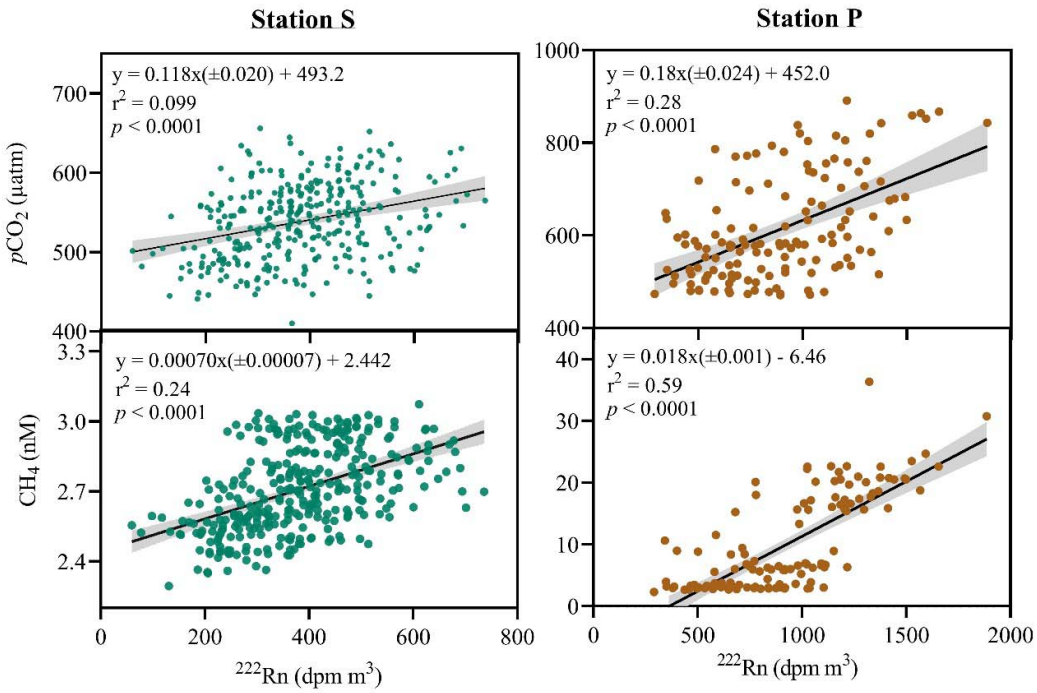

Figure 6. Scatter plot of ^{222}Rn against CH_4 and pCO_2 in Station S (left) and Station P (right). The solid line represents the fitted regression equation, the shaded area are the 95% confidence limits of the regression line, the r^2 value the degree of correlation, and the p value the level of significance.

4.2 Diel pattern in air-sea fluxes of CH_4

A diel air-sea CH_4 pattern with a decreasing trend in afternoon suggests that oxygen availability can control CH_4 emissions to the atmosphere (Figure 3). A 6% to 40% decrease of CH_4 concentrations in the afternoon coinciding with increasing DO and high light intensity indicates higher CH_4 oxidation rate within the water column due to higher oxygen concentration derived from seagrass photosynthesis (Bahlmann et al., 2015) (Figure 7). Increased oxygen from the roots or plant could stimulate aerobic CH_4 oxidation in the water column (Al-Haj & Fulweiler, 2020). Similarly, Lyimo et al., (2018) reported that a reduction of photosynthetic activity result in an increase of CH_4 emissions in a tropical seagrass meadow. Lower air-sea CH_4 emissions in the dense seagrass site (Station S) further demonstrates that photosynthesis could limit CH_4 emissions. The diel CH_4 variation likely implied that the productivity of seagrass drives the oxidation rate of CH_4, controlling CH_4 emissions.

The patchy seagrass contributed to a higher CH_4 flux than the dense seagrass and exhibited a more pronounced CH_4 peak during noon, which was not observed in the dense seagrass. This CH_4 peak could be produced during photosynthesis of submerged photosynthetic organisms as ebullition or through direct CH_4 production, including seagrass, cyanobacteria and algae during (Hilt et al., 2022). The positive correlation of light intensity with CH_4 concentrations observed only in patchy seagrass might suggest abiotic CH_4 photoproduction (Figure 7). A

peak of CH_4 towards noon was also observed in other submerged vegetated habitats such as temperate freshwater marsh in China and a mixed-vegetated habitat in a nearshore bay in the Baltic Sea during summer (Ding et al., 2004; Roth et al., 2022). Moreover, the dead seagrass debris could serve as a source of methylated compounds and stimulate the CH_4 production (Schorn et al., 2022). More studies are needed to understand the contribution of both seagrass meadows and dead matte habitat to CH_4 production.

The high spatial differences in CH_4 concentrations could link to the proximity to the open ocean. The patchy seagrass area had two-times higher ^{222}Rn concentrations and ten-times greater CH_4 fluxes than the area with dense seagrass. As the dense seagrass site was closer to the open ocean, ocean waters could dilute CH_4 concentration within the area, resulting in a lower CH_4 and ^{222}Rn concentrations compared to the more enclosed location of Station P with patchy seagrass (Rosentreter, Borges, et al., 2021).

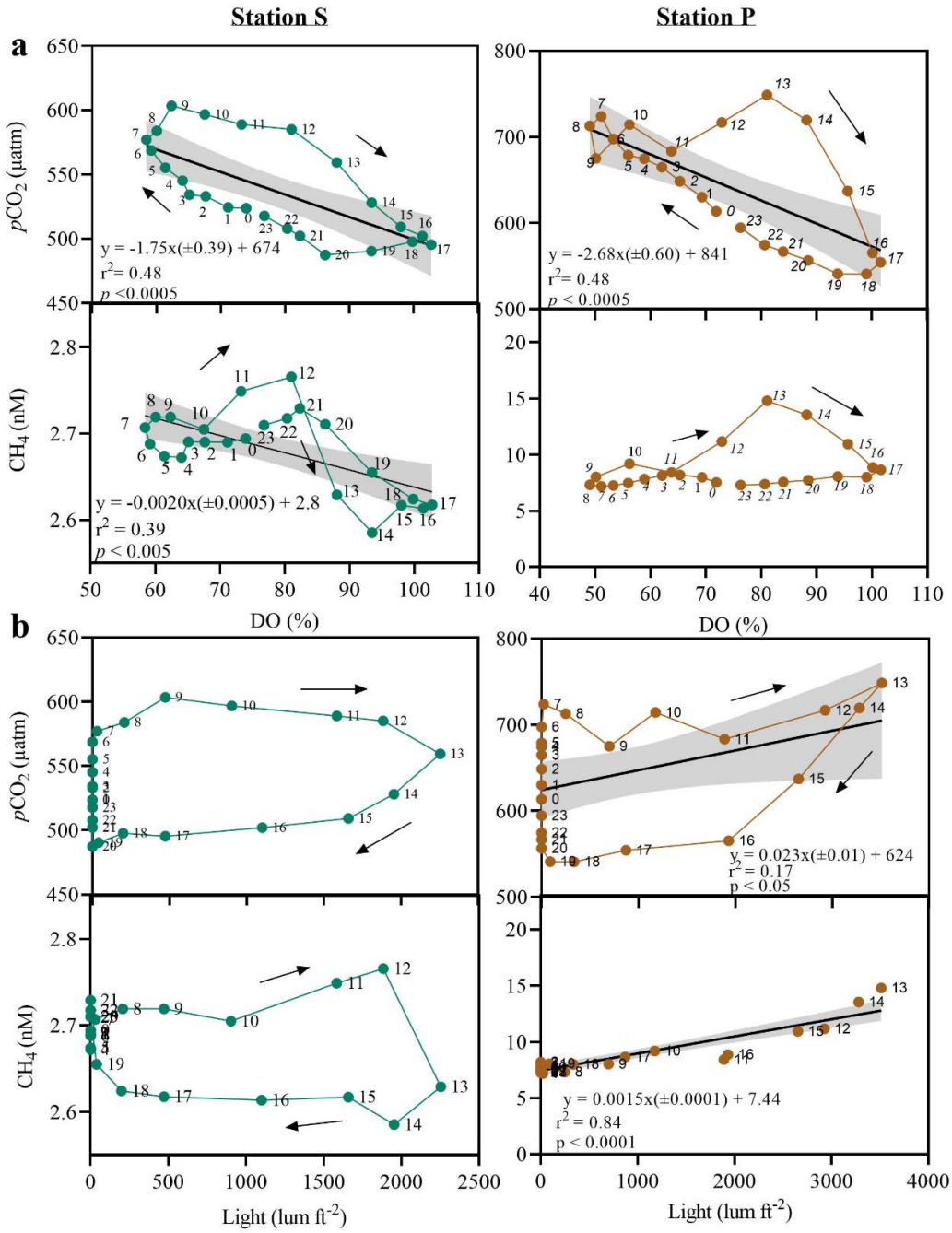

Figure 7. a) Scatter plot of average hourly values of dissolved oxygen (DO) and b) and light intensity against CH_4 and CO_2 in Station S (left) and Station P (right). The solid line represents the fitted regression equation (±SE), and the shaded area are the 95% confidence limits of the regression line, the r^2 value the degree of correlation, and the *p* value the level of significance. The numbers inside the plots indicate the hour of the day. Arrows indicates the hysteresis pattern along the day.

4.3 Low seagrass CH_4 emissions on local and global scales

The average air-sea CH_4 flux (0.12 ± 0.10 µmol CH_4 m^{-2} d^{-1}) estimated are the lowest among seagrass meadows reported to date, which can reach up to 307 µmol CH_4 m^{-2} d^{-1} (Table 4). Our fluxes using the seagrass-derived *k* model from Dobashi and Ho (2022) were 2-11 times lower than other *k* models often used for coastal or open ocean (Borges et al., 2004; Raymond & Cole, 2001; Wanninkhof, 2014). Seagrass meadows attenuate wave energy compared to bare sediment. Therefore, using coastal ocean gas transfer *k* models might overestimate the CH_4 emissions (Table 2). For example, Ollivier et al.(2022) and Banerjee et al. (2018) applied B04 and W14 models, respectively, which partially explains their higher CH_4 emissions.

Another reason for our relatively low CH_4 flux could be the lack of other freshwater sources at our study site. Methane-enriched freshwater inputs could result in overestimates of CH_4 fluxes within seagrass meadows. The air-water CH_4 fluxes from our sites and Australia (Ollivier et al., 2022) (10.6 µmol CH_4 m^{-2} $d^{-}1$) were at the lower end of published data (Table 4). Both studies were located in coastal bays with high salinity and limited tidal or freshwater influence. Our fluxes were two orders of magnitude lower than a brackish lagoon in India (120 µmol CH_4 m^{-2} d^{-1}), and a meso-tidally lagoon in Portugal (307 µmol CH_4 m^{-2} d^{-1}), France and US (Table 4) (Al-Haj et al., 2022; Bahlmann et al., 2015; Banerjee et al., 2018). These other seagrass sites were in tidal systems with freshwater inputs suggesting that the reported high CH_4 fluxes could be partially explained by external freshwater or marsh inputs. This has been observed in other tidally-influenced ecosystems such as mangroves and saltmarshes where higher CH_4 concentration in porewater drives the high surface water CH_4 (Call et al., 2018; Santos et al., 2019; Yau et al., 2022). Flanking saltmarshes adjacent to seagrass export CH_4, elevating CH_4 flux in the seagrass meadows (Al-Haj et al., 2022). Since our system is not directly influenced by flanking marshes, porewater, and freshwater inputs, the relatively low CH_4 air-sea fluxes likely represent emissions from subtidal seagrass habitats.

We combined our results with the literature to re-evaluate global CH_4 emissions from seagrass meadows. It is important to differentiate between sediment-water and air-sea fluxes (Table 4). Fluxes from benthic chamber and sediment core incubation only capture the CH_4 from the sediment to water but do not account for the exchange of CH_4 across the water-air interface or potentially CH_4 oxidation in the water column (Asplund et al., 2022; Bonaglia et al., 2017; Schorn et al., 2022). Our sediment-water fluxes were up to 2 times higher than the air-sea CH_4 fluxes. Earlier global estimates of seagrass CH_4 emissions to the atmosphere (1.25 to 401 µmol CH_4 m^{-2} d^{-1}) were extrapolated from studies using benthic chambers and sediment core incubations (Rosentreter et al. (2021b). Our results show that sediment-water fluxes do not necessarily represent water-air fluxes. Therefore, we updated earlier compilations (Al-Haj et al., 2022) to differentiate between air-sea (8 sites) and sediment-water CH_4 (20 sites) fluxes in seagrass meadows (Table 4). Both air-sea and sediment-water CH_4 fluxes are highly variable. The geometric mean of air-sea and sediment-water CH_4 fluxes (21.6 and 26.1 µmol m^{-2} d^{-1}, respectively) was 3-fold lower than arithmetic mean values (61.6 ± 19.4 and 81.0 ± 19.8 µmol m^{-2} d^{-1}, respectively). The skewed dataset suggests that geometric mean is likely a more realistic representation of fluxes (Williamson & Gattuso, 2022). Overall, previous compilations may have overestimated CH_4 emissions by relying on sediment-water fluxes and mean values rather than air-sea and geometric mean values.

Table 4. *Mean of methane (CH_4) in air-sea and sediment-water fluxes in seagrass reported in the literature.* The mean (± SE), geometric mean and median of air-sea and sediment-water CH_4 fluxes represent the global average.

Location	Species	CH_4 flux ($\mu mol\ m^{-2}\ d^{-1}$)	Site	Method
Water-air				
Chilika Lagoon, India[1]	*Halodule sp. and Halophila sp*	120.0	Tidal lagoon	Water samples
Arcachon Lagoon, France[2]	*Z. noltii*	42.0	Tidal lagoon	Discrete Water samples
Wallagoot, Australia[3]	*R. megacarpa*	33.8	Mouth of estuary	Continous surface water
East Harbor, Massachusetts, USA[4]	*Z. marina*	107.5	Lagoon + marsh	Discrete water samples
Pleasant Bay, Massachusetts,USA[4]	*Z. marina*	113.8	Coastal lagoon	Discrete water samples
Swan Bay, Australia[5]	*Z. mulleri*	10.6	Tidal lagoon	Continous surface water
Cadaques, Spain[6]	*P. oceanica*	0.1	Coastal bay	Continous surface water
	Mean	**61.1 (± 19.4)**		
	Geometric mean	**21.6**		
	Median	**42.0**		
Sediment-water				
Florida, USA[7]	*T. testudinum*	44.0	Coastal lagoon	Benthic chamber
Bimini, Bahamas[7]	*S. filiforme*	5.8	Coastal bay	Benthic chamber
Moreton Bay, Australia[8]	*Z. capricorni*	348.0	Coastal lagoon	Core incubation
Florida, USA[9]	*T. testudinum*	183.4	Coastal lagoon	Benthic chamber
Tomales Bay, USA[10]	*Z. marina*	35.7	Coastal inlet	Benthic chamber
Awerange Bay, Indonesia[11]	*E. acoroides*	95.7	Coastal bay	Benthic chamber
Arcachon Lagoon, France[2]	*Z. noltii*	98.4	Tidal lagoon	Water samples
Ria Formosa Lagoon, Portugal[12]	*Z. noltii*	307.2	Tidal lagoon	Core incubation
Red Sea, Saudi Arabia[13]	*H. uninervis*	48.1	Coastal inlet	Core incubation
Red Sea, Saudi Arabia[13]	*C. serrulata and H. uninervis*	401.3	Coastal inlet	Core incubation
Red Sea, Saudi Arabia[13]	*E. acoroides*	96.2	Coastal inlet	Core incubation
Red Sea, Saudi Arabia[13]	*T. ciliatum*	3.2	Coastal inlet	Core incubation
Red Sea, Saudi Arabia[13]	*H. decipiens*	1.4	Coastal inlet	Core incubation
Red Sea, Saudi Arabia[13]	*T. hemprichii*	6.5	Coastal inlet	Core incubation
Red Sea, Saudi Arabia[13]	*H. stipulacea and H. uninervis*	61.0	Coastal inlet	Core incubation
Chwaka Bay, Tanzania[14]	*T. hemprichii*	74.8	Coastal bay + mangrove	Benthic chamber
Red Sea, Saudi Arabia[15]	*H. stipulacea and H. unervis*	59.7	Coastal lagoon	Core incubation
Virginia, USA[16]	*Z.marina*	136.7	Coastal bay with marsh	Benthic chamber
Mediterranean Sea, Italy[17]	*P. oceanica*	106.0	Coastal bay	Core incubation
Wallis Lake, Australia[3]	*H. ovalis*	45.4	Mouth of estuary	Benthic chamber
Wallis Lake, Australia[3]	*P. australia*	279.3	Mouth of estuary	Benthic chamber
Wallis Lake, Australia[3]	*Z. muelleri*	46.0	Mouth of estuary	Benthic chamber
Wallis Lake, Australia[3]	*Z. muelleri*	10.9	Mouth of estuary	Benthic chamber
Finnland[18]	*Z. marina*	1.6	Coastal bay	Benthic chamber
Denmark[18]	*Z. marina*	3.4	Fjord and coastal bay	Benthic chamber
Sweden[18]	*Z. marina*	2.6	Coastal bay	Benthic chamber
East Harbor, Massachusetts, USA[4]	*Z. marina*	0.0	Back-barrier lagoon	Benthic chamber
Pleasant Bay, Massachusetts,USA[4]	*Z. marina*	73.3	Coastal lagoon	Benthic chamber
Cadaques, Spain[6]	*P. oceanica*	0.3	Coastal bay	Porewater samples
	Mean	**81.0 (± 19.8)**		
	Geometric mean	**26.1**		
	Median	**47.1**		

[1]Banerjee et al., 2018; [2]Deborde et al., 2010; [3]Camillini, 2020; [4]Al-Haj et al., 2022; [5]Ollivier et al., 2022; [6]This study; [7]Oremland, 1975; [8]Moriarty et al., 1984; [9]Barber & Carlson, 1993;

[10]Sansone et al., 1998; [11]Alongi et al., 2008; [12]Bahlmann et al., 2015; [13]Garcias-Bonet, 2017; [14]Lyimo et al., 2018; [15]Burkholz et al., 2020; [16]Oreska et al., 2020; [17]Schorn et al., 2022; [18]Asplund et al., 2022

4.4 Implications for net carbon sequestration

To evaluate the global warming potential of CH_4 emissions in seagrass and the potential offset from carbon burial benefits, air-sea CH_4 fluxes were converted to CO_2-equivalents in 20 and 100 year time horizons using sustained-flux global warming potential (SGWP) of 96 and 45, respectively (Neubauer & Megonigal, 2015). Using different metrics could change the interpretation of the global climatic impact of methane emissions. Our average CH_4 fluxes in Portilligat bay are equivalent to 0.05 and 0.03 g $CO_{2\text{-eq}}$ m^2 yr^{-1} in 20 and 100 year time horizons, respectively. The carbon burial rates from seagrass meadows at our study site have been estimated at 142 ± 69 g C m^{-2} yr^{-1} (Serrano et al., 2016). Therefore, the estimated air-sea CH_4 emissions from *P. oceanica* in our site offset the carbon burial only by < 0.7 % in a 20-year time horizon. The low CH_4 offset is attributed to the low CH_4 flux and high carbon burial of *P. oceanica*. Our average CH_4/CO_2 flux ratio indicate that only about 0.01% of carbon mineralized is emitted as CH_4 (Figure 8).

Global air-sea CH_4 emissions upscaled from the total seagrass area of 160,387 – 266,562 km^2 were 13.0 ± 33.4 Tg $CO_{2\text{-eq}}$ yr^{-1} (4.6 g C m^{-2} yr^{-1}) in 20-year time horizons, which would offset only 1.6% (maximum of 25%) of global seagrass carbon sequestration in soils (833 ± 230 Tg CO_2 yr^{-1} or 138 ± 38 g C m^{-2} yr^{-1}) (Table 5). Yet, both our measurements and the global estimates were mostly conducted across a short period of time. Therefore, long-term CH_4 flux measurements are required to cover the natural variability. Negligible CH_4 offset in both our site and global seagrass averages highlight that seagrasses are significant carbon sinks. Seagrass seems to emit less CH_4 than other coastal vegetated ecosystems such as mangroves and saltmarshes. For example, previous studies showed that methane emissions can offset <6% of carbon burial in a saltmarsh in China (Yau et al., 2022) and 18% in Australian mangroves receiving freshwater inputs (Rosentreter et al., 2018). Since seagrass are fully submerged and freshwater inputs are often limited, higher CH_4 oxidation in the water column could reduce CH_4 emissions relative to periodically inundated mangrove and saltmarsh systems. Overall, our study suggests that seagrass sequesters carbon without emitting large amounts of methane to the atmosphere.

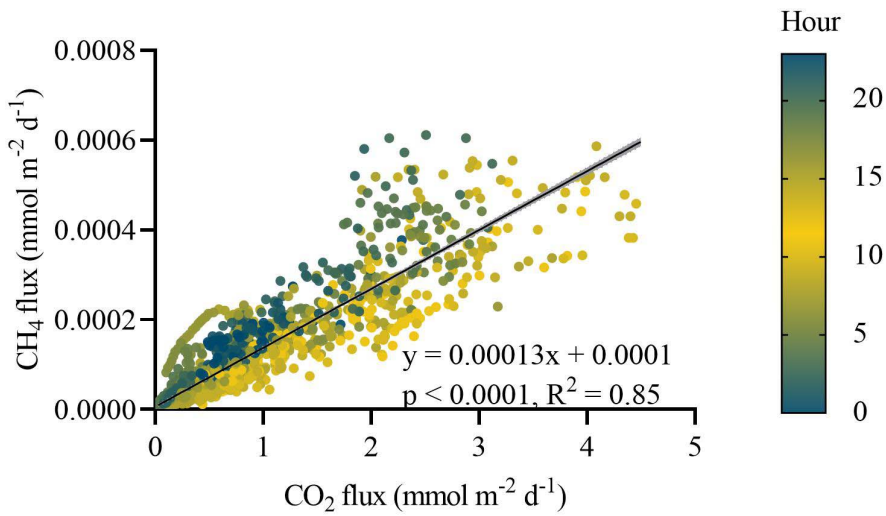

Figure 8. Relationship between CO_2 flux and CH_4 flux in Station S across the study period. The colour represents hour of the day. The solid line represents the fitted regression equation (±SE), and the shaded area are the 95% confidence limits of the regression line, the r^2 value the degree of correlation, and the *p* value the level of significance.

Table 4. *Global CH_4 air-sea and sediment-water emissions estimates from seagrass and the carbon offset.* The CH_4 flux for the seagrass is updated from (Rosentreter, Al-Haj, et al., 2021). *n* refers to number of study sites.

Parameters			Air-sea	Sediment water
n			8	18
CH_4 flux	µmol CH_4 m^{-2} d^{-1}	Geomean[a]	30.1	26.1
	µmol CH_4 m^{-2} d^{-1}	Range	0.1 - 307.2	0.3 - 401.3
Area	km^2	Range	160,387 – 266,562[b]	
Global CH_4 flux	Tg CH_4 yr^{-1}	Mean	0.03	0.02
	Tg CH_4 yr^{-1}	Range	0.00009 - 0.48	0.00028 - 0.62
$SGWP_{100}$	Tg $CO_{2\text{-eq}}$ yr^{-1}	Mean	1.3	1.1
$SGWP_{20}$	Tg $CO_{2\text{-eq}}$ yr^{-1}	Mean	2.7	2.3
Carbon burial*	g C m^{-2} yr^{-1}	Mean + SE	138 ± 38[c]	
	g C m^{-2} yr^{-1}	Range	45 – 190	
Global C burial	Tg C yr^{-1}	Mean + SE	227 ± 63	
Global C burial	Tg CO_2 yr^{-1}	Mean + SE	833 ± 230	
Offset of $SGWP_{100}$	%	Mean	1.6	1.4
	%	Range	0.02 – 11.6	0.05 – 15.1
Offset of $SGWP_{20}$	%	Mean	3.3	2.9
	%	Range	0.03 – 25	0.1 – 32

[a] Global geometric mean was calculated from the global complied data set based on Table 3; [b] Global seagrass area from McKenzie et al., (2020); [c] Global carbon burial was extracted from Mcleod et al., (2011).

5 Conclusion

Our continuous timeseries observations provide new insights into the spatial and diel patterns of CH_4 sediment-water and air-sea fluxes in seagrass-dominated ecosystems. Small CH_4 emissions to the atmosphere were measured in the coastal bay dominated by *P.oceanica*. Porewater profiles reflected methanogenesis activity in deep sediments. The link between ^{222}Rn concentrations and the higher sediment-water to air-sea CH_4 fluxes suggested that sediments were the main source of CH_4 emissions to the atmosphere. CH_4 oxidation in the water column, supported by photosynthesis in seagrass, seem to explain the low CH_4 emissions in the dense seagrass areas. The high spatial variability of CH_4 within the bay highlights the importance of seagrass in regulating CH_4 emissions and/or the dilution by oceanic water. More continuous, high resolution CH_4 measurements are required to resolve the potential diel patterns and the role of seagrass in CH_4 emissions.

Our study highlights the importance of differentiating air-sea and sediment-water flux when estimating seagrass CH_4 emissions. A low CH_4 offset to carbon burial was estimated both on local and global scale seagrass meadows. More site-specific carbon burial and long-term emission estimates are needed to resolve CH_4 dynamics in seagrass carbon budgets. The current evidence suggests minor offsetting of carbon sequestration by seagrass CH_4 emissions.

Acknowledgements

This project was funded by the Swedish Research Council (2020-00457) and Spanish RYC2019-027073-I project. OS was supported by I+D+i project PIE HOLOCENO 20213AT014 funded by MCIN/AEI/10.13039/501100011033 and FEDER. N. P-J. was supported by the Programme for Requalification of the Spanish University System 2021-2023 (Ministerio de Universidades), modality Margarita Salas Grants. We thank the locals from the Portlligat Bay for the boat.

References

Aleksandra, B.-G., & Katarzyna, Ł.-M. (2018). Porewater dissolved organic and inorganic carbon in relation to methane occurrence in sediments of the Gdańsk Basin (southern Baltic Sea). *Continental Shelf Research*, *168*, 11–20. https://doi.org/10.1016/j.csr.2018.08.008

Al-Haj, A. N., Chidsey, T., & Fulweiler, R. W. (2022). Two temperate seagrass meadows are negligible sources of methane and nitrous oxide. *Limnology and Oceanography*, lno.12250. https://doi.org/10.1002/lno.12250

Al-Haj, A. N., & Fulweiler, R. W. (2020). A synthesis of methane emissions from shallow vegetated coastal ecosystems. *Global Change Biology*, *26*(5), 2988–3005. https://doi.org/10.1111/gcb.15046

Alongi, D., Trott, L., Undu, M., & Tirendi, F. (2008). Benthic microbial metabolism in seagrass meadows along a carbonate gradient in Sulawesi, Indonesia. *Aquatic Microbial Ecology*, *51*, 141–152. https://doi.org/10.3354/ame01191

Apostolaki, E. T., Caviglia, L., Santinelli, V., Cundy, A. B., Tramati, C. D., Mazzola, A., & Vizzini, S. (2022). The Importance of Dead Seagrass (Posidonia oceanica) Matte as a Biogeochemical Sink. *Frontiers in Marine Science*, *9*, 861998. https://doi.org/10.3389/fmars.2022.861998

Asplund, M. E., Bonaglia, S., Boström, C., Dahl, M., Deyanova, D., Gagnon, K., Gullström, M., Holmer, M., & Björk, M. (2022). Methane Emissions From Nordic Seagrass Meadow Sediments. *Frontiers in Marine Science*, *8*, 811533. https://doi.org/10.3389/fmars.2021.811533

Bahlmann, E., Weinberg, I., Lavrič, J. V., Eckhardt, T., Michaelis, W., Santos, R., & Seifert, R. (2015). Tidal controls on trace gas dynamics in a seagrass meadow of the Ria Formosa lagoon (southern Portugal). *Biogeosciences*, *12*(6), 1683–1696. https://doi.org/10.5194/bg-12-1683-2015

Banerjee, K., Paneerselvam, A., Ramachandran, P., Ganguly, D., Singh, G., & Ramesh, R. (2018). Seagrass and macrophyte mediated CO2 and CH4 dynamics in shallow coastal waters. *PLOS ONE*, *13*(10), e0203922. https://doi.org/10.1371/journal.pone.0203922

Barber, T. R., & Carlson, P. R. (1993). Effects of Seagrass Die-Off on Benthic Fluxes and Porewater Concentrations of ∑CO2, ∑H2S, and CH4 in Florida Bay Sediments. In *Biogeochemistry of Global Change*. Springer, Boston, MA. https://doi.org/10.1007/978-1-4615-2812-8_29

Bonaglia, S., Brüchert, V., Callac, N., Vicenzi, A., Chi Fru, E., & Nascimento, F. (2017). Methane fluxes from coastal sediments are enhanced by macrofauna. *Scientific Reports*, *13145*, 13145. https://doi.org/10.1038/s41598-017-13263-w

Borges, A. V., & Abril, G. (2011). Carbon Dioxide and Methane Dynamics in Estuaries. In *Treatise on Estuarine and Coastal Science* (pp. 119–161). Elsevier. https://doi.org/10.1016/B978-0-12-374711-2.00504-0

Borges, A. V., Vanderborght, J.-P., Schiettecatte, L.-S., Gazeau, F., Ferrón-Smith, S., Delille, B., & Frankignoulle, M. (2004). Variability of the gas transfer velocity of CO2 in a macrotidal estuary (the Scheldt). *Estuaries*, *27*(4), 593–603. https://doi.org/10.1007/BF02907647

Boudreau, B. P. (1997). *Diagenetic Models and Their Implementation: Modelling Transport and Reactions in Aquatic Sediments*. Springer Berlin Heidelberg. http://catalog.hathitrust.org/api/volumes/oclc/35095947.html

Burkholz, C., Garcias-Bonet, N., & Duarte, C. M. (2020). Warming enhances carbon dioxide and methane fluxes from Red Sea seagrass (<i>Halophila stipulacea</i>) sediments. *Biogeosciences*, *17*(7), 1717–1730. https://doi.org/10.5194/bg-17-1717-2020

Call, M., Sanders, C. J., Enrich-Prast, A., Sanders, L., Marotta, H., Santos, I. R., & Maher, D. T. (2018). Radon-traced pore-water as a potential source of CO2 and CH4 to receding black and clear water environments in the Amazon Basin. *Limnology and Oceanography Letters*, *3*(5), 375–383. https://doi.org/10.1002/lol2.10089

Call, M., Santos, I. R., Dittmar, T., de Rezende, C. E., Asp, N. E., & Maher, D. T. (2019). High pore-water derived CO2 and CH4 emissions from a macro-tidal mangrove creek in the Amazon region. *Geochimica et Cosmochimica Acta*, *247*, 106–120. https://doi.org/10.1016/j.gca.2018.12.029

Camillini, N. (2020). *Carbon and nitrogen cycling in seagrass ecosystems* [Southern Cross University; Application/pdf]. https://researchportal.scu.edu.au/esploro/outputs/doctoral/991012947400202368

Carnell, P. E., Ierodiaconou, D., Atwood, T. B., & Macreadie, P. I. (2020). Overgrazing of Seagrass by Sea Urchins Diminishes Blue Carbon Stocks. *Ecosystems*, *23*(7), 1437–1448. https://doi.org/10.1007/s10021-020-00479-7

Deborde, J., Anschutz, P., Guérin, F., Poirier, D., Marty, D., Boucher, G., Thouzeau, G., Canton, M., & Abril, G. (2010). Methane sources, sinks and fluxes in a temperate tidal Lagoon: The Arcachon lagoon (SW France). *Estuarine, Coastal and Shelf Science*, *89*(4), 256–266. https://doi.org/10.1016/j.ecss.2010.07.013

Ding, W., Cai, Z., & Tsuruta, H. (2004). Diel variation in methane emissions from the stands of Carex lasiocarpa and Deyeuxia angustifolia in a cool temperate freshwater marsh. *Atmospheric Environment*, *38*(2), 181–188. https://doi.org/10.1016/j.atmosenv.2003.09.066

Dobashi, R., & Ho, D. T. (2022). *Air-sea gas exchange in a seagrass ecosystem* [Preprint]. Biogeochemistry: Air - Sea Exchange. https://doi.org/10.5194/egusphere-2022-525

Duarte, C. M., & Krause-Jensen, D. (2017). Export from Seagrass Meadows Contributes to Marine Carbon Sequestration. *Frontiers in Marine Science*, *4*. https://doi.org/10.3389/fmars.2017.00013

Egger, M., Kraal, P., Jilbert, T., Sulu-Gambari, F., Sapart, C. J., Röckmann, T., & Slomp, C. P. (2016). Anaerobic oxidation of methane alters sediment records of sulfur, iron and phosphorus in the Black Sea. *Biogeosciences*, *13*(18), 5333–5355. https://doi.org/10.5194/bg-13-5333-2016

Egger, M., Lenstra, W., Jong, D., Meysman, F. J. R., Sapart, C. J., van der Veen, C., Röckmann, T., Gonzalez, S., & Slomp, C. P. (2016). Rapid Sediment Accumulation Results in High Methane Effluxes from Coastal Sediments. *PLOS ONE*, *11*(8), e0161609. https://doi.org/10.1371/journal.pone.0161609

Fourqurean, J. W., Duarte, C. M., Kennedy, H., Marbà, N., Holmer, M., Mateo, M. A., Apostolaki, E. T., Kendrick, G. A., Krause-Jensen, D., McGlathery, K. J., & Serrano, O. (2012). Seagrass ecosystems as a globally significant carbon stock. *Nature Geoscience*, *5*(7), 505–509. https://doi.org/10.1038/ngeo1477

Froelich, P. N., Klinkhammer, G. P., Bender, M. L., Luedtke, N. A., Health, G. R., Cullen, D., Dauphin, P., Hammond, D., Hartman, B., & Maynard, V. (1979). Early oxidation of organic matter in pelagic sediments of the eastern equatorial Atlantic: Suboxic diagenesis. *Geochimica et Cosmochimica Act*, *43*(7).

Gacia, E., Duarte, C. M., & Middelburg, J. J. (2002). Carbon and nutrient deposition in a Mediterranean seagrass (*Posidonia oceanica*) meadow. *Limnology and Oceanography*, *47*(1), 23–32. https://doi.org/10.4319/lo.2002.47.1.0023

Garcias-Bonet, N. (2017). Methane Production by Seagrass Ecosystems in the Red Sea. *Frontiers in Marine Science*, *4*, 10.

Heiri, O., Lotter, A. F., & Lemcke, G. (2001). Loss on ignition as a method for estimating organic and carbonate content in sediments: Reproducibility and comparability of results. *Journal of Paleolimnology*, *25*(1), 101–110.

Hilt, S., Grossart, H., McGinnis, D. F., & Keppler, F. (2022). Potential role of submerged macrophytes for oxic methane production in aquatic ecosystems. *Limnology and Oceanography*, lno.12095. https://doi.org/10.1002/lno.12095

Hoehler, T. M., Borowski, W. S., Alperin, M. J., Rodriguez, N. M., & Paull, C. K. (2000). *Model, stable isotope, and radiotracer characterization of anaerobic methane oxidation in gas hydrate-bearing sediments of the Blake ridge* (C. K. Paull, R. Matsumoto, P. J. Wallace, & W. P. Dillon, Eds.; Vol. 164). Proc. ODP, Sci. https://doi.org/10.2973/odp.proc.sr.164.2000

Kaal, J., Serrano, O., del Río, J. C., & Rencoret, J. (2018). Radically different lignin composition in Posidonia species may link to differences in organic carbon sequestration capacity. *Organic Geochemistry*, *124*, 247–256. https://doi.org/10.1016/j.orggeochem.2018.07.017

Kennedy, H., Beggins, J., Duarte, C. M., Fourqurean, J. W., Holmer, M., Marbà, N., & Middelburg, J. J. (2010). Seagrass sediments as a global carbon sink: Isotopic constraints: SEAGRASS MEADOWS AS CARBON SINKS. *Global Biogeochemical Cycles*, *24*(4), n/a-n/a. https://doi.org/10.1029/2010GB003848

Leiva-Dueñas, C., López-Merino, L., Serrano, O., Martínez Cortizas, A., & Mateo, M. A. (2018). Millennial-scale trends and controls in Posidonia oceanica (L. Delile) ecosystem productivity. *Global and Planetary Change*, *169*, 92–104. https://doi.org/10.1016/j.gloplacha.2018.07.011

Lengier, M., Szymczycha, B., Brodecka-Goluch, A., Kłostowska, Ż., & Kuliński, K. (2021). Benthic diffusive fluxes of organic and inorganic carbon, ammonium and phosphates from deep water sediments of the Baltic Sea. *Oceanologia*, *63*(3), 370–384. https://doi.org/10.1016/j.oceano.2021.04.002

Lerman, A. (1979). *Geochemical processes water and sediment environment*. John Wiley and Sons.

Li, L. (2021). Interspecific differences in root exudation for three tropical seagrasses and sediment pore-water dissolved organic carbon beneath them. *Marine Pollution Bulletin*, 8.

Lo Iacono, C., Mateo, M. A., Gràcia, E., Guasch, L., Carbonell, R., Serrano, L., Serrano, O., & Dañobeitia, J. (2008). Very high-resolution seismo-acoustic imaging of seagrass meadows (Mediterranean Sea): Implications for carbon sink estimates. *Geophysical Research Letters*, *35*(18), L18601. https://doi.org/10.1029/2008GL034773

Lovelock, C. E., & Duarte, C. M. (2019). Dimensions of Blue Carbon and emerging perspectives. *Biology Letters*, *15*(3), 20180781. https://doi.org/10.1098/rsbl.2018.0781

Lyimo, L. D., Gullström, M., Lyimo, T. J., Deyanova, D., Dahl, M., Hamisi, M. I., & Björk, M. (2018). Shading and simulated grazing increase the sulphide pool and methane emission in a tropical seagrass meadow. *Marine Pollution Bulletin*, *134*, 89–93. https://doi.org/10.1016/j.marpolbul.2017.09.005

Martens, C. S., & Klump, M. J. (1980). Biogeochemical cycling in an organic-rich coastal marine basin—I. Methane sediment-water exchange processes. *Geochimica et Cosmochimica Acta*, 471–490.

Mateo, M. A., Romero, J., Pérez, M., Littler, M. M., & Littler, D. S. (1997). Dynamics of Millenary Organic Deposits Resulting from the Growth of the Mediterranean SeagrassPosidonia oceanica. *Estuarine, Coastal and Shelf Science*, *44*(1), 103–110. https://doi.org/10.1006/ecss.1996.0116

McKenzie, L. J., Nordlund, L. M., Jones, B. L., Cullen-Unsworth, L. C., Roelfsema, C., & Unsworth, R. K. F. (2020). The global distribution of seagrass meadows. *Environmental Research Letters*, *15*(7), 074041. https://doi.org/10.1088/1748-9326/ab7d06

Mcleod, E., Chmura, G. L., Bouillon, S., Salm, R., Björk, M., Duarte, C. M., Lovelock, C. E., Schlesinger, W. H., & Silliman, B. R. (2011). A blueprint for blue carbon: Toward an improved understanding of the role of vegetated coastal habitats in sequestering CO_2. *Frontiers in Ecology and the Environment*, *9*(10), 552–560. https://doi.org/10.1890/110004

Moriarty, D. J. W., Boon, P. I., Hansen, J. A., Hunt, W. G., Poiner, I. R., & Pollard, P. C. (1984). Microbial biomass and productivity in seagrass beds. *Geomicrobiology Journal*, *4*(1), 21–51.

Neubauer, S. C., & Megonigal, J. P. (2015). Moving Beyond Global Warming Potentials to Quantify the Climatic Role of Ecosystems. *Ecosystems*, *18*(6), 1000–1013. https://doi.org/10.1007/s10021-015-9879-4

Ollivier, Q. R., Maher, D. T., Pitfield, C., & Macreadie, P. I. (2022). Net Drawdown of Greenhouse Gases (CO2, CH4 and N2O) by a Temperate Australian Seagrass Meadow. *Estuaries and Coasts*. https://doi.org/10.1007/s12237-022-01068-8

Oremland, R. S. (1975). Methane Production in Shallow-Water, Tropical Marine Sediments. *APPL. MICROBIOL.*, *30*, 7.

Oreska, M. P. J., McGlathery, K. J., Aoki, L. R., Berger, A. C., Berg, P., & Mullins, L. (2020). The greenhouse gas offset potential from seagrass restoration. *Scientific Reports*, *10*(1), 7325. https://doi.org/10.1038/s41598-020-64094-1

Piñeiro-Juncal, N., Kaal, J., Moreira, J. C. F., Martínez Cortizas, A., Lambais, M. R., Otero, X. L., & Mateo, M. A. (2021). Cover loss in a seagrass Posidonia oceanica meadow accelerates soil organic matter turnover and alters soil prokaryotic communities. *Organic Geochemistry*, *151*, 104140. https://doi.org/10.1016/j.orggeochem.2020.104140

Raymond, P., & Cole, J. (2001). Gas Exchange in Rivers and Estuaries: Choosing a Gas Transfer Velocity. *Estuaries and Coasts*, *24*, 312–317. https://doi.org/10.2307/1352954

Rosentreter, J. A., Al-Haj, A. N., Fulweiler, R. W., & Williamson, P. (2021). Methane and Nitrous Oxide Emissions Complicate Coastal Blue Carbon Assessments. *Global Biogeochemical Cycles*, *35*(2). https://doi.org/10.1029/2020GB006858

Rosentreter, J. A., Borges, A. V., Deemer, B. R., Holgerson, M. A., Liu, S., Song, C., Melack, J., Raymond, P. A., Duarte, C. M., Allen, G. H., Olefeldt, D., Poulter, B., Battin, T. I., & Eyre, B. D. (2021). Half of global methane emissions come from highly variable aquatic ecosystem sources. *Nature Geoscience*, *14*(4), 225–230. https://doi.org/10.1038/s41561-021-00715-2

Rosentreter, J. A., Maher, D. T., Erler, D. V., Murray, R. H., & Eyre, B. D. (2018). Methane emissions partially offset “blue carbon” burial in mangroves. *Science Advances*, *4*(6), eaao4985. https://doi.org/10.1126/sciadv.aao4985

Roth, F., Sun, X., Geibel, M. C., Prytherch, J., Brüchert, V., Bonaglia, S., Broman, E., Nascimento, F., Norkko, A., & Humborg, C. (2022). High spatiotemporal variability of methane concentrations challenges estimates of emissions across vegetated coastal ecosystems. *Global Change Biology*, gcb.16177. https://doi.org/10.1111/gcb.16177

Sansone, F. J., Rust, T. M., & Smith, S. V. (1998). Methane Distribution and Cycling in Tomales Bay, California. *Estuaries*, *21*(1), 66. https://doi.org/10.2307/1352547

Santos, I. R., Maher, D. T., Larkin, R., Webb, J. R., & Sanders, C. J. (2019). Carbon outwelling and outgassing vs. Burial in an estuarine tidal creek surrounded by mangrove and saltmarsh wetlands. *Limnology and Oceanography*, *64*(3), 996–1013. https://doi.org/10.1002/lno.11090

Schorn, S., Ahmerkamp, S., Bullock, E., Weber, M., Lott, C., Liebeke, M., Lavik, G., Kuypers, M. M. M., Graf, J. S., & Milucka, J. (2022). Diverse methylotrophic methanogenic archaea cause high methane emissions from seagrass meadows. *Proceedings of the National Academy of Sciences*, *119*(9), e2106628119. https://doi.org/10.1073/pnas.2106628119

Serrano, O., Almahasheer, H., Duarte, C. M., & Irigoien, X. (2018). Carbon stocks and accumulation rates in Red Sea seagrass meadows. *Scientific Reports*, *8*(1), 15037. https://doi.org/10.1038/s41598-018-33182-8

Serrano, O., Gómez-López, D. I., Sánchez-Valencia, L., Acosta-Chaparro, A., Navas-Camacho, R., González-Corredor, J., Salinas, C., Masque, P., Bernal, C. A., & Marbà, N. (2021). Seagrass blue carbon stocks and sequestration rates in the Colombian Caribbean. *Scientific Reports*, *11*(1), 11067. https://doi.org/10.1038/s41598-021-90544-5

Serrano, O., Lavery, P. S., López-Merino, L., Ballesteros, E., & Mateo, M. A. (2016). Location and Associated Carbon Storage of Erosional Escarpments of Seagrass Posidonia Mats. *Frontiers in Marine Science*, *3*. https://doi.org/10.3389/fmars.2016.00042

Serrano, O., Mateo, M. A., Renom, P., & Julià, R. (2012). Characterization of soils beneath a Posidonia oceanica meadow. *Geoderma*, *185–186*, 26–36. https://doi.org/10.1016/j.geoderma.2012.03.020

Telesca, L., Belluscio, A., Criscoli, A., Ardizzone, G., Apostolaki, E. T., Fraschetti, S., Gristina, M., Knittweis, L., Martin, C. S., Pergent, G., Alagna, A., Badalamenti, F., Garofalo, G., Gerakaris, V., Louise Pace, M., Pergent-Martini, C., & Salomidi, M. (2015). Seagrass meadows (Posidonia oceanica) distribution and trajectories of change. *Scientific Reports*, *5*(1), 12505. https://doi.org/10.1038/srep12505

Van Dam, B., Polsenaere, P., Barreras-Apodaca, A., Lopes, C., Sanchez-Mejia, Z., Tokoro, T., Kuwae, T., Loza, L. G., Rutgersson, A., Fourqurean, J., & Thomas, H. (2021). Global Trends in Air-Water CO_2 Exchange Over Seagrass Meadows Revealed by Atmospheric Eddy Covariance. *Global Biogeochemical Cycles*, *35*(4). https://doi.org/10.1029/2020GB006848

Wanninkhof, R. (2014). Relationship between wind speed and gas exchange over the ocean revisited. *Limnology and Oceanography: Methods*, *12*(6), 351–362. https://doi.org/10.4319/lom.2014.12.351

Ward, B. B., Kilpatrick, K. A., Novellit, P. C., & Scrantont, M. I. (1987). Methane oxidation and methane fluxes in the ocean surface layer and deep anoxic waters. *Nature*, 4.

Webb, J. R., Maher, D. T., & Santos, I. R. (2016). Automated, in situ measurements of dissolved CO2 , CH4 and δ 13C values using cavity enhanced laser absorption spectrometry: Comparing response times of air-water equilibrators: Equilibrator measurement of dissolved CO2 , CH4 , and δ13 C values. *Limnology and Oceanography: Methods*, *14*(5), 323–337. https://doi.org/10.1002/lom3.10092

Weber, T., Wiseman, N. A., & Kock, A. (2019). Global ocean methane emissions dominated by shallow coastal waters. *Nature Communications*, *10*(1), 4584. https://doi.org/10.1038/s41467-019-12541-7

Weiss, R. F. (1974). Carbon dioxide in water and seawater: The solubility of a non-ideal gas. *Marine Chemistry*, *2*(3), 203–215. https://doi.org/10.1016/0304-4203(74)90015-2

Williamson, P., & Gattuso, J.-P. (2022). Carbon Removal Using Coastal Blue Carbon Ecosystems Is Uncertain and Unreliable, With Questionable Climatic Cost-Effectiveness. *Frontiers in Climate*, *4*, 853666. https://doi.org/10.3389/fclim.2022.853666

Yamamoto, S., Alcauskas, J. B., & Crozier, T. E. (1976). Solubility of methane in distilled water and seawater. *Journal of Chemical & Engineering Data*, *21*(1), 78–80. https://doi.org/10.1021/je60068a029

Yau, Y. Y. Y., Xin, P., Chen, X., Zhan, L., Call, M., Conrad, S. R., Sanders, C. J., Li, L., Du, J., & Santos, I. R. (2022). Alkalinity export to the ocean is a major carbon sequestration mechanism in a macrotidal saltmarsh. *Limnology and Oceanography*, lno.12155. https://doi.org/10.1002/lno.12155

Automatic citation updates are disabled. To see the bibliography, click Refresh in the Zotero tab.